

Which nanowire couples better electrically to a metal contact: Armchair or zigzag nanotube?

M. P. Anantram^{a)}

NASA Ames Research Center, Mail Stop T27A-1, Moffett Field, California 94035-1000

(Received 28 November 2000; accepted for publication 7 February 2001)

The fundamental question of how chirality affects the electronic coupling of a nanotube to metal contacts is important for the application of nanotubes as nanowires. We show that metallic-zigzag nanotubes are superior to armchair nanotubes as nanowires, by modeling the metal–nanotube interface. More specifically, we show that as a function of coupling strength, the total electron transmission of armchair nanotubes increases and tends to be pinned close to unity for a metal with Fermi wave vector close to that of gold. In contrast, the total transmission of zigzag nanotubes increases to the maximum possible value of two. The origin of these effects lies in the details of the wave function, which is explained. © 2001 American Institute of Physics.

[DOI: 10.1063/1.1360228]

The chirality of a nanotube is of prime importance in determining its electronic properties. Chirality determines whether a nanotube is metallic or semiconducting.¹ Ref. 2 showed that the band gap change with tensile and torsional strain has a rather universal dependence on nanotube chirality. The electronic properties of zigzag and armchair nanotubes (two distinct chiralities) are also affected in very different manners upon bending.³ From the viewpoint of nanotubes in applications such as nanowires, it is critical to understand the physics of metal–nanotube coupling. We find that the overlap between nanotube and metal wave functions depend significantly on chirality.

We consider a single wall carbon nanotube coupled to a metal block in the side-contacted geometry (Fig. 1). The metal contact is treated in the context of a free electron metal with a rectangular cross section in the (x,z) plane, and infinite extent in the y direction as in most experiments. The surface Green's function of the metal contact is calculated using standard procedures. The nanotube is treated using the π orbital tight binding Hamiltonian. The coupling between the metal and the nanotube is modeled using a tunneling-type Hamiltonian, which is included to all orders (and not just Born approximation) in calculating the transmission probability. The details of modeling the metal–nanotube coupling can be found in Ref. 4. The total transmission (T) is defined to be the sum over the transmission probability of all modes at an energy. T at energy E is given by,⁵ $T(E) = \text{Tr}[G^r(E)\Gamma_m(E)G^a(E)\Gamma_c(E)]$, where Γ_m and Γ_c are matrices that represent coupling between the metal and a semi-infinite nanotube region either to the left- or right-hand side of the nanotube section shown in Fig. 1. G^r (G^a) is the full retarded (advanced) Green's function of the nanotube with coupling to metal and semi-infinite nanotube regions included.

The coupling strength of the metal contact to the nanotube is given by the diagonal component of Γ_m which is $|t_{mc}|^2\rho_m$, where ρ_m is the density of states of the metal sur-

face and t_{mc} represents the hopping strength between nanotube atoms and metal in the Hamiltonian.⁴ The electrical contact length (Fig. 1) between the metal and nanotube in this work is dictated by the available computational resources. The largest electrical contact length considered is thirty nanotube unit cells (approximately 72 and 125 Å for armchair and zigzag nanotubes, respectively). The dimensions of the metal contact are $L_x=400\text{--}750\text{ Å}$ and $L_z=750\text{ Å}$. The length of nanotube–metal electrical contact is kept constant at thirty nanotube unit cells, and the transmission is calculated as a function of coupling strength ($|t_{mc}|^2\rho_m$). Three values of metal Fermi wave vector (k_f) are considered, 1.75 Å^{-1} (aluminum), 1.2 Å^{-1} (gold/silver) and 0.9 Å^{-1} , where free electron metals with k_f close to the assumed values are indicated in the parentheses.

Figure 2 shows the transmission probability as a function of coupling strength for a (5,5) armchair nanotube. The results show the dramatic effect that T is pinned close to unity for $k_f=1.2$ and 0.9 Å^{-1} . Close to the Fermi energy (nanotube band center), two subbands carry current in both the positive and negative directions. This result indicates that only one of the two subbands couples well to the metal. For $k_f=1.75$, T is well above unity, implying that both subbands

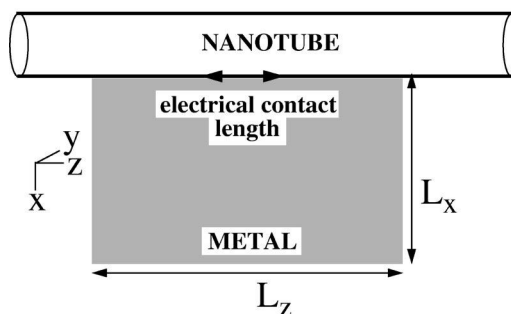


FIG. 1. Nanotube lying on a metal contact. The metal contact is infinitely long in the y direction (open boundaries), and thirty unit cells of the nanotube make electrical contact to the metal. Semi-infinite nanotube regions present to the left- and right-hand side of the nanotube section are not shown. The total transmission (T) is evaluated from the metal to either the semi-infinite nanotube region to the left- or right-hand side.

^{a)}Electronic mail: anantr@nas.nasa.gov

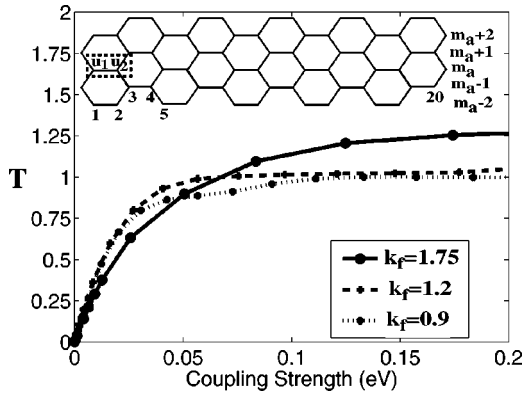


FIG. 2. Plot of T vs coupling strength between metal and armchair nanotube. While for $k_f = 0.9$ and 1.2 \AA^{-1} , T is pinned close to unity, for $k_f = 1.75 \text{ \AA}^{-1}$, T is larger.

couple to the metal. The wave functions of the crossing bands of the two positive going states of a (N,N) armchair nanotube are⁶

$$\begin{aligned}\phi_{ac1} &= e^{im_a k_a a_0/2} (-1)^{m_a} [1 \ 1] \\ \phi_{ac2} &= e^{im_a k_a a_0/2} (-1)^{m_a} [1 \ -1],\end{aligned}\quad (1)$$

where k_a is the axial wave vector of the nanotube, m_a is an integer that denotes the cross section along the axial direction (inset of Fig. 2), and $(u_1 \ u_2)$ is the wave function of a unit cell of the underlying graphene sheet. For an armchair nanotube, there is *no modulation* of $(u_1 \ u_2)$ around the circumferential direction. The wave function of one of the two subbands (ϕ_{ac2}) is rapidly oscillating with antinodes separated by 1.4 \AA . In comparison, the nodes of a metal wave function (ϕ_m) with $k_f = 0.9, 1.2$ and 1.75 \AA^{-1} , are separated by $6.3, 3.4$, and 2 \AA , respectively, taking into account that the axial wave vector has to be at least 0.75 \AA^{-1} .⁴ As a result of this, the integral entering the Born approximation for scattering rate,

$$\int \phi_{ac2}^* H_{c-m} \phi_m \quad (2)$$

(H_{c-m} is the nanotube-metal coupling Hamiltonian), is very small for $k_f = 0.9$ and 1.2 \AA^{-1} , and is larger for $k_f = 1.75 \text{ \AA}^{-1}$, in that order. Thus, T is pinned close to unity for $k_f = 0.9$ and 1.2 \AA^{-1} , and is larger for $k_f = 1.75 \text{ \AA}^{-1}$.⁷ Recently, an alternate mechanism by which only one of the two crossing subbands of an armchair nanotube contributes to transport was discussed in Ref. 8. The nanotube can be divided into regions where the nanotube atoms make and do not make contact to the metal atoms. A shift in the band structure between these two regions by about 1.5 eV causes a reflection of electrons incident from the metal into one of the two crossing subbands, at the interface between the two regions, as proposed in Ref. 8. Our work includes such a shift but in comparison to Ref. 8, we find that the conductance can be around unity (for $k_f = 0.9$ and 1.2 \AA^{-1}) even when this shift is smaller than 1.5 eV . Also, we propose that the crossing subband with the smaller angular momentum contributes more significantly to transport.

Figure 3 shows the metal-nanotube total transmission (T) as a function of coupling strength for a (6,0) zigzag nanotube. In stark contrast to the armchair case, T does not satu-

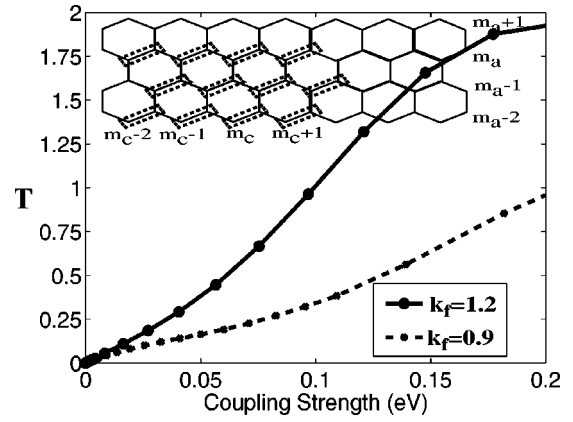


FIG. 3. Plot of T vs coupling strength between metal and zigzag nanotube. In contrast to the armchair case, T increases to the maximum allowed value of two with coupling strength.

rate at unity. With increasing coupling strength, T approaches two, the maximum value possible. That is, both positive going subbands contribute to transmission from metal to nanotube. The wave function of the two crossing subbands of a zigzag nanotube are

$$\phi_{zz1} = e^{(-i\sqrt{3}m_a k_a a_0)/2} e^{i2\pi m_a/3} e^{i4\pi m_c/3} [u_1 \ u_2]$$

and

$$\phi_{zz2} = e^{(-i\sqrt{3}m_a k_a a_0)/2} e^{i4\pi m_a/3} e^{i8\pi m_c/3} [u_1 \ u_2], \quad (3)$$

where, m_a is an integer that denotes the cross section along the axial direction and m_c is an integer denoting the various unit cells along the circumferential direction as shown in Fig. 3. The wave function along the circumferential direction varies much more slowly than the armchair wave function:

$$\phi_{zz}(m_a, m_c) + \phi_{zz}(m_a, m_c + 1) + \phi_{zz}(m_a, m_c + 2) = 0, \quad (4)$$

which corresponds to a distance of $2a_0$ over which the wave function adds up to zero. As a result of this feature [Eq. (4)], both crossing subbands of a zigzag nanotube couple with metals. In Figs. 2 and 3, it is noted that for small coupling strengths, T is larger for the armchair nanotube than the zigzag nanotube case. This is because as a result of the small circumferential wave vector of ϕ_{ac1} , ϕ_{ac1} couples more strongly to the metal than the sum of contributions from ϕ_{zz1} and ϕ_{zz2} . With increasing coupling strengths, both crossing subbands of the zigzag nanotube however eventually couple well to the metal, unlike the armchair nanotube.

The calculations presented consider the entire circumference of the nanotube to be coupled to the metal contact. Such a scenario is relevant to the experiment in Ref. 9, which resulted in a conductance of approximately $2e^2/h$. Other experiments involve the metal making contact to only part of the circumference of the nanotube.¹⁰ We also perform calculations corresponding to this case. The number of atoms around the nanotube circumference that couple to the metal contact is shown in the legend of Fig. 4. While the difference between a four (even) and five (odd) atom sector is negligible in the zigzag case, it is larger for the armchair case (note the difference in slope). The reason for this, based on the discussion of scattering rate within the Born approximation is that the end odd atom (Fig. 2) corresponding to the

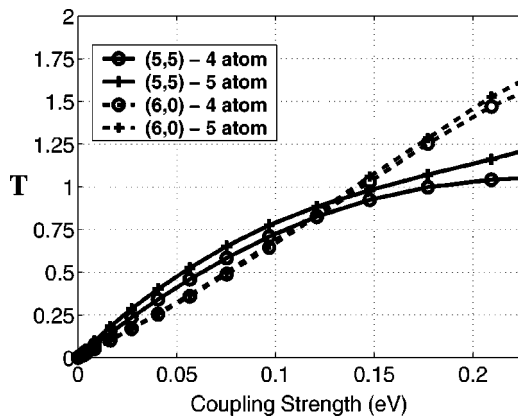


FIG. 4. Plot of T vs coupling strength between metal and nanotube for the case of a sector of the nanotube circumference making contact to the metal. The legend shows the number of contiguous atoms (see inset of Fig. 2) in a unit cell making contact. The essential features of Figs. 2 and 3 are retained. The metal Fermi wave vector was chosen to be close to that of gold (1.2 \AA^{-1}).

wave function ϕ_{ac2} does not have a partner-atom to compensate (to make zero) its contribution to the scattering rate in Eq. (2).

Two practical issues, disorder/defects and length dependence, are discussed next. A ten percent random variation in coupling strength between the nanotube atoms and the metal does not cause a significant change in the results. A very large disorder in coupling will cause both modes of the armchair nanotube to couple equally well to the metal. Defects in the nanotube such as the Stone–Wales defect will be more effective in destroying the discussed difference.

The transmission probability of an electron from the metal to the nanotube can be made larger either by increasing the coupling strength or by increasing the area of electrical contact, between the nanotube and metal. From a technological perspective, the first alternative of small contact area (as assumed in this letter) along with strong coupling is more desirable. In typical experiments, the coupling between metal and nanotube is weak compared to the 0.2 eV assumed for the largest coupling in Figs. 2 and 3, and the contact length is larger. The results of this letter are also qualitatively valid for a calculation where the coupling strength is constant and the electrical contact length is increased (“coupling strength” in the x axis of Figs. 2–4 should be replaced by electrical contact length). In the case of armchair nanotubes, the state with larger angular momentum (which couples weakly to the metal) will eventually contribute to conductance as the contact length is made very large. The increase in conductance with contact length is however expected to be slow once the state with smaller angular momentum has coupled to the metal.

Many factors such as the role of curvature, torsion and tension of armchair, and zigzag nanotubes play a role in determining the suitability of nanotubes as nanowires. The small curvature induced band gap in large diameter metallic-zigzag nanotubes predicted by tight-binding theory is smaller than kT .¹ Further, Ref. 11 showed that a (6,0) nanotube is a perfect metal, contrary to the popular belief that all small diameter metallic-zigzag nanotubes have a small band gap. This lends support to the use of metallic-zigzag nanotubes as nanowires. In this letter, we considered the role of the electron wave function of the nanotube in determining the coupling strength to a metal contact, in the absence of significant defects. We find that zigzag nanotubes perform better than armchair nanotubes as nanowires. For Fermi wave vectors close to that of gold, the total transmission (T) of side-contacted armchair tubes is pinned close to unity. In contrast, the total transmission in case of zigzag tubes is close to the maximum possible value of two. This represents a two fold increase in the small bias current that can be driven through a zigzag nanotube when compared to an armchair nanotube. The case of disorder in coupling and long contact lengths were commented upon.

The author would like to thank Supriyo Datta for useful discussions.

- ¹N. Hamada, S. Sawada, and A. Oshiyama, Phys. Rev. Lett. **68**, 1579 (1992); R. Saito, M. Fujita, G. Dresselhaus, and M. S. Dresselhaus, Appl. Phys. Lett. **60**, 2204 (1992).
- ²L. Yang, M. P. Anantram, J. Han, and J. P. Lu, Phys. Rev. B **60**, 13874 (1999).
- ³M. B. Nardelli and J. Bernholc, Phys. Rev. B **60**, R16338 (1999); A. Rochefort, P. Avouris, F. Lesage, and D. R. Salahub, Phys. Rev. B **60**, 13824 (1999).
- ⁴M. P. Anantram, S. Datta, and Y. Xue, Phys. Rev. B **61**, 14219 (2000).
- ⁵S. Datta, *Electronic Transport in Mesoscopic Systems* (Cambridge University Press, Cambridge, UK, 1995).
- ⁶P. R. Wallace, Phys. Rev. **71**, 622 (1947).
- ⁷S. Datta (private communication), came to a similar conclusion of wave function overlaps based on a Bessel function approach.
- ⁸H. J. Choi, J. Ihm, Y.-G. Yoon, and S. G. Louie, Phys. Rev. B **60**, 14009 (1999).
- ⁹S. Frank, P. Poncharal, Z. L. Wang, and W. A. de Heer, Science **280**, 1744 (1998); P. Poncharal, S. Frank, Z. L. Wang, and W. A. de Heer, Eur. Phys. J. D **9**, 77 (1999).
- ¹⁰S. J. Tans, M. Devoret, H. Dai, A. Thess, R. E. Smalley, L. J. Geerligs, and C. Dekker, Nature (London) **386**, 474 (1997); D. H. Cobden, M. Bockrath, P. L. McEuen, A. G. Rinzler, and R. E. Smalley, Phys. Rev. Lett. **81**, 681 (1998); R. Martel, T. Schmidt, H. R. Shea, T. Hertel, and P. Avouris, Appl. Phys. Lett. **73**, 2447 (1998); P. J. de Pablo, E. Graugnard, B. Walsh, R. P. Andres, S. Datta, and R. Reifengerger, Appl. Phys. Lett. **74**, 323 (1999); C. Schonenberger, A. Bachtold, C. Strunk, J.-P. Salvetat, and L. Forro, Appl. Phys. A: Mater. Sci. Process. **A69**, 283 (1999).
- ¹¹X. Blase, L. X. Benedict, E. L. Shirley, and S. G. Louie, Phys. Rev. Lett. **72**, 1878 (1994).